

Analysis of Chromatin Regulators Reveals Specific Features of Rice DNA Methylation Pathways¹

Feng Tan², Chao Zhou², Qiangwei Zhou², Shaoli Zhou, Wenjing Yang, Yu Zhao, Guoliang Li, and Dao-Xiu Zhou*

National Key Laboratory of Crop Genetic Improvement, Huazhong Agricultural University, 430070 Wuhan, China (F.T., C.Z., Q.Z., S.Z., W.Y., Y.Z., G.L., D.-X.Z.); and Institute of Plant Sciences Paris-Saclay, Centre National de la Recherche Scientifique, Institut National de la Recherche Agronomique, Université Paris-Saclay, Université Paris-sud 11, 91405 Orsay, France (D.-X.Z.)

ORCID IDs: 0000-0001-9111-1598 (S.Z.); 0000-0003-4451-9907 (Y.Z.); 0000-0002-1540-0598 (D.-X.Z.).

Plant DNA methylation that occurs at CG, CHG, and CHH sites (H = A, C, or T) is a hallmark of the repression of repetitive sequences and transposable elements (TEs). The rice (*Oryza sativa*) genome contains about 40% repetitive sequence and TEs and displays specific patterns of genome-wide DNA methylation. The mechanism responsible for the specific methylation patterns is unclear. Here, we analyzed the function of OsDDM1 (Deficient in DNA Methylation 1) and OsDRM2 (Deficient in DNA Methylation 2) in genome-wide DNA methylation, TE repression, small RNA accumulation, and gene expression. We show that OsDDM1 is essential for high levels of methylation at CHG and, to a lesser extent, CG sites in heterochromatic regions and also is required for CHH methylation that mainly locates in the genic regions of the genome. In addition to a large number of TEs, loss of OsDDM1 leads to hypomethylation and up-regulation of many protein-coding genes, producing very severe growth phenotypes at the initial generation. Importantly, we show that OsDRM2 mutation results in a nearly complete loss of CHH methylation and derepression of mainly small TE-associated genes and that OsDDM1 is involved in facilitating OsDRM2-mediated CHH methylation. Thus, the function of OsDDM1 and OsDRM2 defines distinct DNA methylation pathways in the bulk of DNA methylation of the genome, which is possibly related to the dispersed heterochromatin across chromosomes in rice and suggests that DNA methylation mechanisms may vary among different plant species.

DNA methylation in flowering plants occurs in three sequence contexts: the so-called symmetric CG and CHG and the asymmetric CHH, where H is any nucleotide except G. Methylation in each context is believed to be catalyzed primarily by a specific family of DNA methyltransferases: MET1 (homologous to animal Dnmt1) for CG, plant-specific chromomethylases (CMT3 and CMT2) for CHG, and DRM2 (homologous to animal Dnmt3) for CHH (Law and Jacobsen, 2010).

Recently, it was shown that CMT2 is a major CHH methyltransferase in Arabidopsis (*Arabidopsis thaliana*; Zemach et al., 2013; Stroud et al., 2014). The majority of plant methylation is found in transposable elements (TEs) and transcribed TE genes (known as transposable element-related genes [TEGs]) and is crucial for the repression of TE expression and transposition (Law and Jacobsen, 2010). Substantial methylation also is found in the bodies of active genes, where methylation is generally restricted to the CG context (Law and Jacobsen, 2010; Zemach et al., 2010). Methylation in all sequence contexts also is found in the promoter regions of many genes, which represses gene expression.

In Arabidopsis, the maintenance of CHH methylation is mediated by RNA-directed DNA methylation (RdDM) involving the methyltransferase activity of DRM2 (Law and Jacobsen, 2010). DNA methylation also is influenced by chromatin factors. For instance, the Arabidopsis Snf2 family nucleosome remodeler DDM1, which can shift nucleosomes in vitro (Brzeski and Jerzmanowski, 2003), is essential for normal DNA methylation (Jeddeloh et al., 1999; Lippman et al., 2004). The loss of DDM1 leads to a profound decrease of methylation from some TEs and repeats and strong transcriptional activation of TEs (Jeddeloh et al., 1999; Lippman et al., 2004), and inbred *ddm1* mutant lines have increased rates of transposition and produce severe developmental abnormalities (Tsukahara et al.,

¹ This work was supported by the National Natural Science Foundation of China (grant nos. 31371241 and 31571256), the National High Technology Research and Development Program of China (grant no. 2014AA10A600), the French Agence Nationale de la Recherche (Nerdpah), and the Huazhong Agricultural University Scientific and Technological Self-Innovation Foundation (grant no. 2016RC003).

² These authors contributed equally to the article.

* Address correspondence to dao-xiu.zhou@u-psud.fr.

The author responsible for distribution of materials integral to the findings presented in this article in accordance with the policy described in the Instructions for Authors (www.plantphysiol.org) is: Dao-Xiu Zhou (dao-xiu.zhou@u-psud.fr).

F.T. analyzed the OsDDM1 genes and mutants; C.Z. analyzed the OsDRM2 gene and mutant; Q.Z. did the bioinformatic analysis; S.Z., W.Y., and Y.Z. did the H3K27me3 and H3K9me2 chromatin immunoprecipitation sequencing; D.-X.Z., F.T., C.Z., and Q.Z. analyzed the data and wrote the article.

www.plantphysiol.org/cgi/doi/10.1104/pp.16.00393

2009). Mutation of *Lsh*, the mouse homolog of DDM1, causes similar methylation phenotypes (Tao et al., 2010). Recent data indicate that Arabidopsis DDM1 is important for DNA methylation in TEs, and the strength of the DDM1 requirement is positively correlated with heterochromatin (Zemach et al., 2013). It is believed that DDM1 can facilitate CMT2-mediated CHH methylation independently of RdDM and that DDM1 and RdDM synergistically mediate nearly all Arabidopsis TE methylation, prevent transposition, and maintain proper patterns of gene expression (Zemach et al., 2013).

Rice (*Oryza sativa*) is one of the most important food crops in the world and has been established as a model plant for genome research. The rice genome, one of the most accurately sequenced eukaryotic genomes, contains about 40% repetitive sequence and TEs (Paterson et al., 2009). In contrast to the more localized pattern of repeats close to centromeres in Arabidopsis, repeats in rice are widely spread on the chromosomes. In addition, the rice genome contains a large number of miniature inverted-repeat transposable elements (MITEs), a majority of which are associated with genes (Feschotte and Wessler, 2002; Lu et al., 2012). Extensive genome-wide DNA methylation and histone modification data sets have been generated in rice (Feng et al., 2010; He et al., 2010; Zemach et al., 2010; Li et al., 2012; Liu et al., 2015). Compared with Arabidopsis, the rice genome displays a different global DNA methylation profile and has a much higher level of genome-wide cytosine methylation (Feng et al., 2010; Li et al., 2012). Rice genes involved in DNA methylation are generally conserved (Chen and Zhou, 2013), and some of them have been studied. For instance, knockdown of *OsDRM2* by homologous recombination-mediated gene targeting produces very severe defects at the seedling stage (Moritoh et al., 2012). Except for *OsMET1* (Hu et al., 2014), the function of rice methylation genes in genome-wide DNA methylation is unknown. In particular, it is unclear whether a similar mechanism is conserved for the bulk of methylation of the rice genome that displays significant structural differences from that of Arabidopsis.

Here, we report a genome-wide analysis of DNA methylation, gene expression, and small RNA abundance in rice plants lacking *OsDDM1* and *OsDRM2*. We find that loss of *OsDDM1* and *OsDRM2* severely affects rice plant growth in the initial generation and causes the deregulation of a large number of genes, indicating an essential role of the proteins in maintaining proper patterns of gene expression in rice. We find that *OsDDM1* is required for heterochromatic CHG and CG methylation and euchromatic CHH methylation. We find that, in contrast to Arabidopsis *DRM2*, which is required for a minor part of CHH methylation of the genome, *OsDRM2* is required for most of the CHH methylation in rice, which is essentially located in small TEs such as MITEs that are scattered in the genic regions. Importantly, we find that

OsDDM1-mediated CHH methylation sites totally overlapped with that by *OsDRM2*, suggesting that *OsDDM1* may be involved in *OsDRM2*-mediated CHH methylation. These data revealed specific pathways that mediate the bulk of genomic DNA methylation in rice, suggesting that specific epigenetic mechanisms may be elaborated to adapt to genome structure variation that is strikingly high in plants.

RESULTS

OsDDM1 Genes Are Required Mainly for Heterochromatic CHG and CG Methylation and Euchromatic CHH Methylation

Rice has two *DDM1* homologous genes, *OsDDM1a* (Os09g27060) and *OsDDM1b* (Os03g51230), which share 93% amino acid identity (Higo et al., 2012). Both genes displayed a similar expression pattern, with the transcript levels of *OsDDM1b* higher than that of *OsDDM1a* in the tested organs (Supplemental Fig. S1A). A previous study showed that down-regulation of both genes by antisense produced a dwarf phenotype in the transgenic plants, some of which progressively lost fertility and became completely infertile (Higo et al., 2012). Here, we isolated homozygous loss-of-function transfer DNA (T-DNA) insertion mutants of the two genes (Supplemental Fig. S1, B and C). However, the single *osddm1a* or *osddm1b* mutation did not produce any clear phenotype during either the vegetative or reproductive stage, even after several generations (Supplemental Fig. S1D). By contrast, the *osddm1a/1b* double mutation obtained by genetic crosses produced many severe developmental abnormalities, including an extremely reduced plant height at the mature stage and complete sterility (Fig. 1A; Supplemental Fig. S1E), suggesting that the two rice *DDM1* orthologs acted redundantly to ensure normal plant growth and development. To study the effects of the mutations on DNA methylation, we first estimated overall methylated cytosine levels by mass spectrometry (MS). The analysis revealed that the *osddm1a* and *osddm1b* single mutations reduced cytosine methylation by 3% and 11.5%, respectively, whereas the *osddm1a/1b* double mutation reduced the methylation by 53.6% (Supplemental Table S1). The synergistic effects on phenotype production and cytosine methylation suggested that the two genes had a redundant function in cytosine methylation and gene regulation. To study the precise effects on genome-wide DNA methylation, we generated single-nucleotide resolution maps of cytosine methylation in seedling leaf tissues of *osddm1a*, *osddm1b*, and the double mutants by bisulfite sequencing (BS-seq; Supplemental Table S2). Because the rice T-DNA mutants were obtained after callus culture, in this work we used callus culture-regenerated wild-type plants as a control. Compared with the wild type, methylation at CG, CHG, and CHH sites in *osddm1a* was reduced by 5.5%, 14%, and 18.9%, respectively,

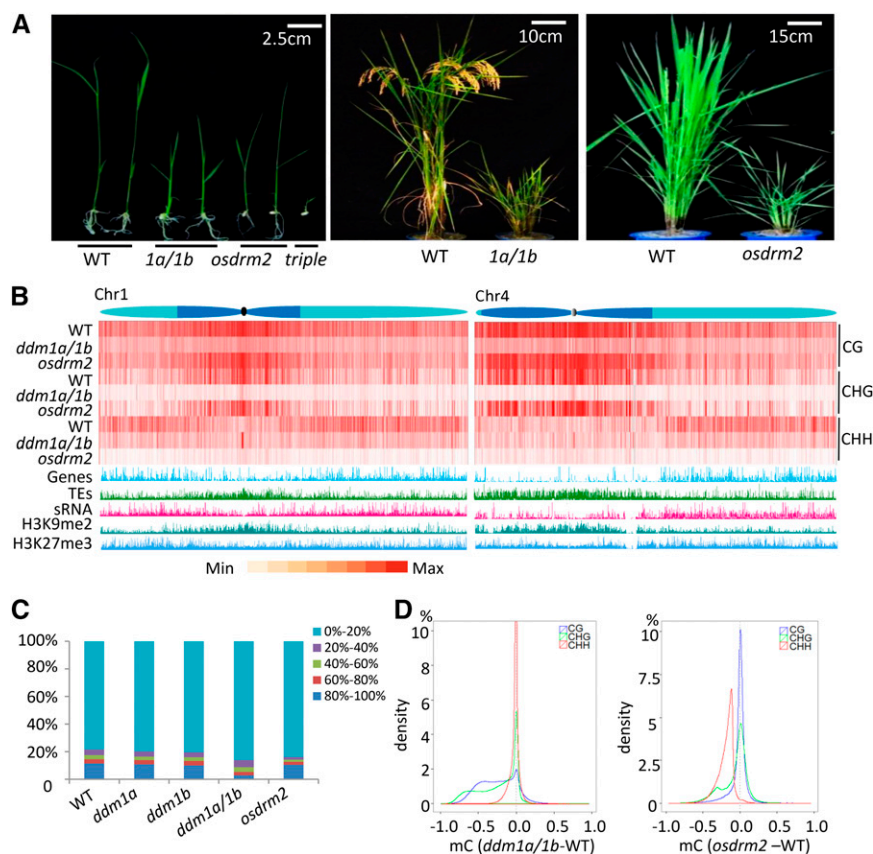


Figure 1. Effects of the *osddm1a/1b* and *osdrm2* mutations on plant growth and genome-wide cytosine methylation. A, The *osddm1a/1b* and *osdrm2* mutations severely reduced plant height. Plants at seedling and mature stages are shown. The *osddm1a/1b osdrm2* triple mutants were seedling lethal. B, Heat map of methylation levels at CG, CHG, and CHH sites in chromosomes 1 and 4 of the wild type (WT), *osddm1a/1b*, and *osdrm2*. Average methylation levels per 1-kb bin were calculated and are shown as red bars. The distribution of histones H3K9me2 and H3K27me3 and small interfering RNA (siRNAs) identified in this work are shown along the chromosomes. Genes and TEs are indicated. The heterochromatin (dark blue) and euchromatin (light blue) regions of the chromosomes are drawn according to Cheng et al. (2001). C, Effects of *osdrm2* and *osddm1a/1b* mutations on cytosine methylation at different levels. Genome-wide cytosine methylation is divided into five intervals (from lowest [0%–20%] to highest [80% or greater], represented by the indicated colors). The percentage of each interval (detected in the wild type and the mutants) is shown on the y axis. D, Density plots of differential methylation levels at CG (blue), CHG (green), and CHH (red) sites in *osddm1* (left) and *osdrm2* (right) compared with the wild type. The y axis shows the percentage of differential methylation levels, and the x axis shows differential methylation levels (from -1 to $+1$) in the mutants relative to the wild type (0), with the area of each sequence context set as 100%. Only methylation differences for 1-kb windows containing at least five informative sequenced cytosines were considered.

while that in *osddm1b* was reduced by 8.3%, 26%, and 32%, respectively. The double mutation caused 44.9%, 73.5%, and 49% reductions of CG, CHG, and CHH methylation, respectively (Table I). More dramatic losses of CHG and CG than CHH methylation were found in the double mutant, suggesting that the two rice *DDM1* orthologs functioned redundantly to mostly regulate CHG and CG methylation. However, it is possible that deregulation of methylation-related genes or disrupted methylation homeostasis might account for the divergence in CHG/CG and CHH methylation changes between single and double mutants.

In rice chromosomes, the majority of heterochromatin is distributed in the pericentromeric regions, with chromosome 4 having a distinct pattern in which the

entire left (short) arm is highly heterochromatinized (Cheng et al., 2001; Fig. 1B). We observed that methylation at CG and CHG sites was enriched in heterochromatic regions, whereas CHH methylation was located essentially in euchromatic regions (Fig. 1B). For comparison, we analyzed genome-wide H3K9me2 (a heterochromatic gene mark), H3K27me3 (a euchromatic gene mark; Supplemental Table S3), and small RNAs in the same tissues as for BS-seq of wild-type plants. H3K9me2 was relatively more enriched in the heterochromatic and pericentromeric regions, while more peaks of H3K27me3 were found in euchromatic regions (Fig. 1B). siRNA also was enriched in the euchromatic region in rice, consistent with previous observations in maize (*Zea mays*; Gent et al., 2014). The

Table 1. Cytosine methylation levels in wild-type and mutant plants

Genotype	Methylation Levels				Percentage of Decrease			
	C	CG	CHG	CHH	C	CG	CHG	CHH
Wild type	17.60%	63.90%	30.60%	5.30%				
<i>ddm1a</i>	15.90%	60.40%	26.30%	4.30%	9.66%	5.48%	14.05%	18.87%
<i>ddm1b</i>	14.70%	58.60%	22.60%	3.60%	16.48%	8.29%	26.14%	32.08%
<i>osdrm2</i>	12.60%	57.00%	23.60%	0.80%	28.41%	10.80%	22.88%	84.91%
<i>ddm1a/1b</i>	8.10%	35.20%	8.10%	2.70%	53.98%	44.91%	73.53%	49.06%

analysis revealed that the *osddm1a/1b* double mutation resulted in predominant losses of CHG and, to a lesser extent, CG methylation, mostly in heterochromatin regions, and clear CHH methylation losses in euchromatic regions of the chromosomes (Fig. 1B), suggesting that OsDDM1 is involved in the methylation of both heterochromatic and euchromatic regions of the genome.

OsDRM2 Is Required for Most of the CHH Methylation in Rice

The rice genome contains three *DRM1/2* homologous genes. *OsDRM2* (Os03g0110800) is the major *DRM1/2*-type methyltransferase gene in rice, as *OsDRM1a* (Os11g0109200) and *OsDRM1b* (Os12g01018900) are not expressed and/or lack methyltransferase motifs (Moritoh et al., 2012). To study the function of *OsDRM2* in DNA methylation, we characterized a homozygous T-DNA insertion mutant of the gene (Supplemental Fig. S1, B and C). This mutant displayed severe pleiotropic growth phenotypes at both the vegetative and reproductive stages, including a dwarfed stature, reduction in tiller number, delayed heading or no heading, abnormal panicle and spikelet morphology, and complete sterility, which are similar to the previously characterized *osdrm2* knockout plants (Fig. 1A; Supplemental Fig. S1E; Moritoh et al., 2012). Analysis of the single-nucleotide resolution maps of cytosine methylation of seedling leaves by BS-seq revealed that the *osdrm2* mutation greatly reduced CHH methylation (84.9%), but with much weaker effects on CG (10.8%) and CHG (22.9%) methylation (Table 1). As in the *osddm1a/1b* double mutant, losses of CHH methylation in *osdrm2* plants were located primarily in euchromatin domains (Fig. 1B), suggesting that OsDRM2 may play an important role in gene regulation.

To study the characteristics of methylated cytosines targeted by OsDDM1 and OsDRM2, we divided the cytosine methylation levels into five intervals (20% each from 0% to 100%) and calculated the percentages of each interval in the wild type and mutants. The analysis revealed that the *osddm1a/1b* double mutation preferentially reduced the percentage of the highest interval (greater than 80% methylation; Fig. 1C), indicating that OsDDM1 mostly targeted to heavily methylated regions of the genome. By contrast, the

osdrm2 mutation mainly reduced the percentages of moderately methylated intervals (20%–40% and 40%–60% methylation; Fig. 1C). To further refine the methylation losses at each sequence context in the mutants, we plotted the percentage (density) of the methylation changes (from -1 to $+1$) in the mutants relative to the wild type (set at 0) at CG, CHG, and CHH sites. The analysis indicated that the areas of heavy CHG and CG methylation losses (greater than 50%; from -0.5 to -1) were much larger than that of CHH methylation in *osddm1a/1b* (Fig. 1D). In contrast, in *osdrm2*, CHH methylation losses were most prevalent (e.g. about 75% at -0.2), while CG methylation loss was not clearly observed (Fig. 1D). This analysis confirmed the above observations that OsDDM1 was mainly required for CHG and CG methylation, whereas OsDRM2 was essentially required for CHH methylation.

Function of OsDDM1 and OsDRM2 in DNA Methylation of Protein-Coding Genes

To study the effects of the mutations on methylation levels at different genomic elements, we calculated the percentages of methylated cytosines of each of the rice protein-coding genes, TEGs, and TEs and plotted them according to the length of each element. This analysis indicated that the rice protein-coding genes had lower methylation levels than TEs and TEGs (Fig. 2; Supplemental Fig. S2). Like TEs or TEGs, a small group of protein-coding genes displayed high levels of CG methylation (greater than 80%; Fig. 2A; Supplemental Fig. S2). The *osddm1a/1b* double mutation eliminated the high level of CG methylation and reduced CHG and CHH methylation in protein-coding genes (Fig. 2A). To analyze the mutation effects on methylation levels at different regions of rice protein-coding genes, we calculated the average methylation levels for every 100-bp interval of each gene and its 2-kb upstream and downstream flank regions in wild-type and mutant plants. The analysis revealed that, in the wild type, CG methylation was at about similar levels between the 5' and 3' regions and gene body (except the ends of the body), while non-CG methylation was much higher in the 5' and 3' regions than the body (Fig. 2B), confirming previous data (Zemach et al., 2010). In *osddm1a/1b*, CHG and CHH methylation was reduced mainly from the 5' and 3' regions of protein-coding genes (Fig. 2B). By

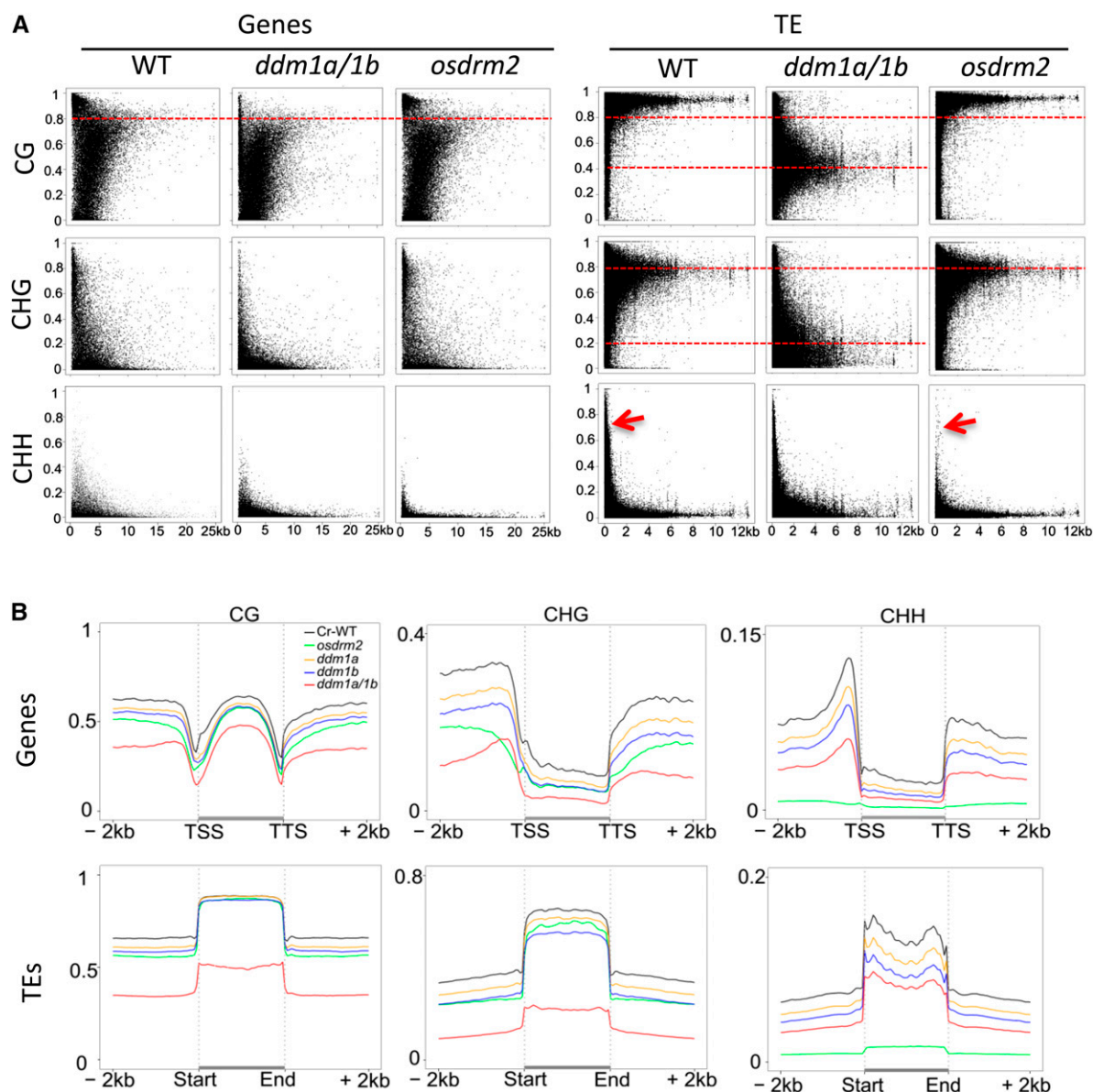


Figure 2. Average cytosine methylation levels in all sequence contexts in genes and TEs. A, Average cytosine methylation levels in all sequence contexts plotted against gene (left) and TE (right) sizes. Note that high levels of wild-type (WT) CG methylation (greater than 80%) in genes and TEs were reduced to about 40% on average in *osddm1a/1b*, and wild-type CHG levels (80% on average) in TEs were reduced to lower levels (about 20% on average) in *osddm1a/1b* but remained unchanged in *osdrm2*, which mostly reduced CHH methylation in genes and small TEs (less than 1 kb; arrows). The percentage of methylated cytosines out of total cytosines of each protein-coding gene or TE was plotted in terms of the lengths of the elements. Each dot represents a gene or TE. B, Patterns and genome-wide average levels of cytosine methylation (CG, CHG, and CHH) of genes (top row) and TEs (bottom row) in wild-type and mutant rice plants. Protein-coding genes and TEs with their contiguous 2-kb upstream and downstream flanks were aligned at the 5' and 3' ends, and average cytosine methylation levels within each 100-bp interval are plotted.

contrast, the *osdrm2* mutation largely reduced CHH methylation (Fig. 2A), which was located mostly at the 5' and 3' ends of protein-coding genes (Fig. 2B). *McrBC* digestion and PCR analysis of methylation levels of several genes confirmed the BS-seq data (Supplemental Fig. S3). This analysis indicated that both OsDDM1 and OsDRM2 were mainly involved in methylation of the 5' and 3' ends of protein-coding genes.

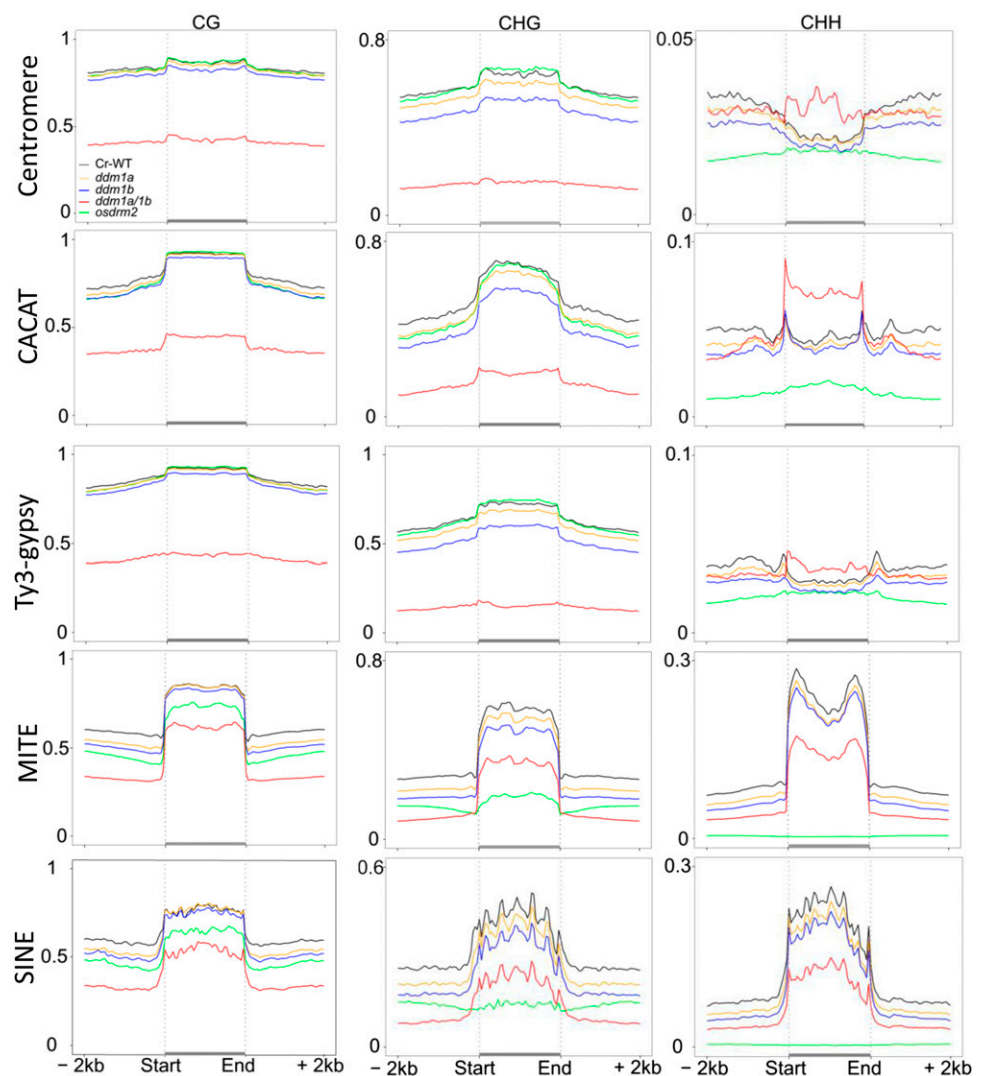
Function of OsDDM1 in TE and TEG Methylation

TE and repetitive sequences represent about 40% of the rice genome. In addition, the rice genome contains a large number of TEGs (16,924, compared with 38,622 protein-coding genes; <http://rice.plantbiology.msu.edu/>). Similar analysis to that with the protein-coding genes revealed that rice TEs and TEGs were highly

methylated at CG and CHG sites, but only small TEs (less than 1 kb) showed relatively high levels of CHH methylation (Fig. 2A; Supplemental Fig. S2). In *osddm1a/1b* plants, CHG and CG methylation in TEs and TEGs were greatly reduced (Fig. 2; Supplemental Fig. S2). However, CG methylation reduction (from an average of more than 80% to about 40%) appeared less important than that of CHG methylation (from about 80% to about or below 20%) of long TEs and TEGs (Fig. 2A; Supplemental Fig. S2). Consistent with the observation in Figure 1B, these data indicated that OsDDM1 was required predominantly for CHG methylation. *McrBC* digestion and PCR analysis of four TEGs confirmed the BS-seq data (Supplemental Fig. S3). Analysis of average cytosine methylation levels within each 100-bp interval of the different classes of TEs and repeats revealed hyper-CHH methylation of centromere repeats, CACAT DNA elements, and long terminal repeat retrotransposons (Ty3-gypsy) in *osddm1a/1b* plants (Fig. 3; Supplemental Fig. S4). Hyper-CHH

methylated TEs were located mostly in the pericentromeric regions (Supplemental Fig. S5). The ectopic CHH methylation may be caused by an internal balancing mechanism to compensate for the extensive loss of CHG and CG methylation found in heterochromatic TEs due to the loss of OsDDM1 function. Considering that DRM2 or RdDM seems not to be required for CHH methylation of heterochromatic or long TEs in Arabidopsis and maize (Zemach et al., 2013; Li et al., 2014), the ectopic CHH methylation in heterochromatic TEs may be mediated by a CMT2-like activity that was shown to methylate CHH in heterochromatic regions in Arabidopsis (Zemach et al., 2013). However, the *osddm1a/1b* mutation clearly reduced CHH methylation of small TEs (i.e. MITEs and SINEs; Fig. 3). Thus, OsDDM1 was required mainly for CHG and, to a lesser extent, CG methylation of TEs and TEGs. OsDDM1 also was required for CHH methylation of small TEs, which are located mainly in the euchromatic region (see below).

Figure 3. Genome-wide average levels of methylation in each sequence context of the indicated TE families and repeats in culture-regenerated wild-type (Cr WT) and mutant plants. TEs with their contiguous 2-kb upstream and downstream flanks were aligned at the 5' and 3' ends, and average methylation for all cytosines within each 100-bp interval is plotted. Note the hyper-CHH methylation of centromere repeats, CACAT, and Ty3-gypsy retroelements in *osddm1a/1b* plants and the nearly complete losses of CHH and CHG methylation of MITEs and short interspersed nuclear elements (SINEs) in *ordm2* plants.



OsDRM2 Is Required for CHH Methylation of Gene-Associated Small TEs

The *osdrm2* mutation clearly reduced CHH methylation of TEs, especially small TEs (less than 1 kb), but had little effect on CG or CHG methylation of TEs or TEGs (Fig. 2; Supplemental Fig. S2). When we examined the methylation levels of different classes of TEs, we found that the *osdrm2* mutation generally reduced CHH methylation of TEs, but it almost completely eliminated CHH methylation from small TEs such as MITEs and SINEs (Fig. 3; Supplemental Fig. S4). This is consistent with the function of Arabidopsis DRM2 (Tran et al., 2005). Small TEs, especially MITEs, are the most abundant short DNA elements in rice and are dispersed in genic regions (Bureau and Wessler, 1994; Zemach et al., 2010). MITEs are located at high frequencies at the 5' and 3' ends of protein-coding genes (Fig. 4A). MITEs are highly methylated at CHH sites in different rice tissues, and MITE distribution closely parallels that of CHH methylation (Zemach et al., 2010). In *osdrm2* plants, CHH methylation losses peaked at the 5' and 3' ends of protein-coding genes (Fig. 4B). We found that about 28% (15,484 of 55,546) of the total rice genes had MITE sequences detected within the range from 200 bp upstream to 200 bp downstream to the coding regions (Fig. 4C). About 71% (9,750 of 13,673) of the hypo-CHH methylated genes (see below) in *osdrm2* were MITE-associated genes (Fig. 4C). Analysis by *Mcr*BC and *Hae*III digestion coupled with PCR of MITE-associated genes confirmed the BS-seq data (Supplemental Fig. S3). Thus, OsDRM2-dependent CHH methylation mainly targets gene-associated small TEs, thereby affecting the methylation of protein-coding genes.

OsDDM1-Dependent CHH Methylation Sites Overlap with That Methylated by OsDRM2

Next, we analyzed differentially methylated cytosines (DMCs), differentially methylated regions (DMRs), and

differentially methylated genes (DMGs) in all sequence contexts (see "Materials and Methods") and found that the *ddm1a/1b* double mutation mostly produced hypomethylated DMCs or DMRs at CHG and, to a lesser extent, at CHH and CG sites, while the *osdrm2* mutation produced hypomethylated DMCs/DMRs essentially at CHH sites (Fig. 5A; Supplemental Table S5). Relatively smaller numbers of hypermethylated CHH DMCs/DMRs also were produced in *osddm1a/1b* plants (Fig. 5A). In terms of DMGs, the *osddm1a/1b* mutation produced not only a large number of hypo-CHG methylated TEGs (about 8,600) but also many hypo-CHG (about 2,500) and hypo-CHH (about 6,000) methylated protein-coding genes (Fig. 5A; Supplemental Table S5). The *osdrm2* mutation produced about 11,700 hypo-CHH methylated protein-coding genes (Fig. 5A; Supplemental Table S5). These data indicated that OsDDM1 and OsDRM2 controlled the methylation of many functional genes in rice, suggesting that they might play an important role in gene regulation.

Hypo-DMRs at CG and CHG sites in *osddm1a/1b* had lower H3K27me3 but higher H3K9me2 levels than the genome-wide average, while hypo-CHH DMRs in both *osddm1a/1b* and *osdrm2* plants displayed higher H3K27me3 and lower H3K9me2 than the genome-wide average (Fig. 5B). These data were consistent with the above observations that CHH methylation losses in both *osddm1a/1a* and *osdrm2* plants were located essentially in euchromatic regions and that CHG methylation losses in *osddm1a/1b* were mainly in heterochromatic regions (Fig. 1B). Interestingly, nearly all of the hypo-CHH DMRs in *osddm1a/1b* were overlapped by those in *osdrm2* (Fig. 5C), while there was little overlap of hypo-CG or hypo-CHG DMRs between the two mutants (Fig. 5C). We observed that the wild-type methylation levels of the overlapped regions were higher than the regions affected only in *osdrm2* (Fig. 5D). The overlapped

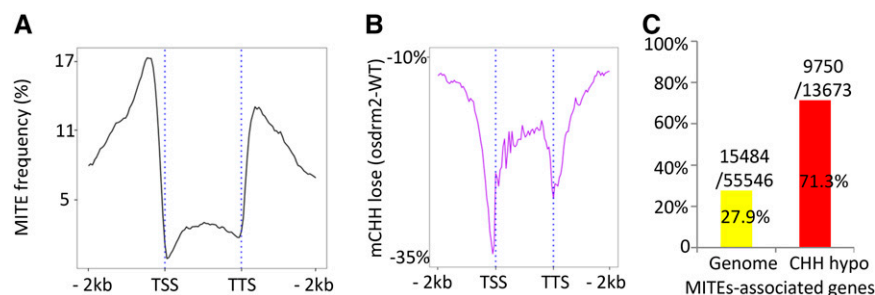
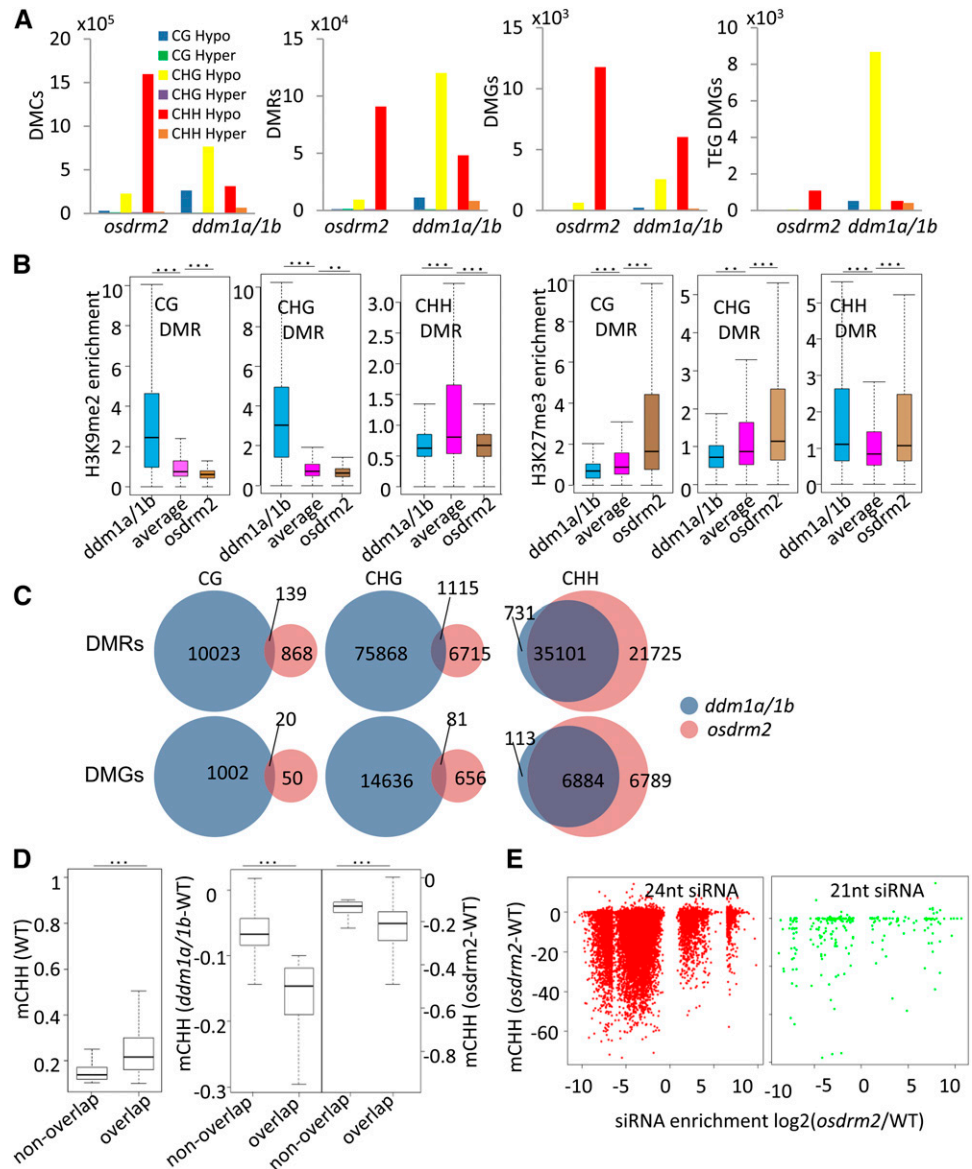


Figure 4. The *osdrm2* mutation reduces CHH methylation of MITEs that are located close to genes. A, Frequency of the occurrence of MITEs in rice protein-coding genes. The rice protein-coding genes (including the body and the 2-kb upstream and downstream regions) were divided into 120 intervals (x axis) and searched for the presence of MITE sequences at each interval. The y axis shows the percentage of rice genes with the presence of MITEs. B, Distribution of genome-wide average losses of CHH methylation in the rice protein-coding genes in *osdrm2*. All rice protein-coding genes (including the body and the 2-kb upstream and downstream regions) were divided into 120 intervals (x axis), and CHH methylation losses at each interval in *osdrm2* compared with the wild type (WT) are shown as minus percentages (y axis). C, High enrichment of MITE-associated genes in hypo-CHH methylation (71.4%) in *osdrm2*, compared with 27.9% of MITE-associated genes genome wide. TSS, Transcription start site; TTS: transcription terminal site.

Figure 5. Analysis of DMCs, DMRs, and DMGs detected in *osddm1a/1b* and *osdrum2* mutants. A, Numbers of hypo- and hyper-DMCs/DMRs/DMGs detected in *osddm1a/1b* and *osdrum2*. DMGs of protein-coding genes and TEGs are shown. B, Enrichment of H3K9me2 or H3K27me3 of hypo-CG, -CHG, and -CHH DMRs in *osddm1a/1b* and *osdrum2* plants relative to genome-wide averages. Significant enrichments are indicated by double asterisks ($P < 0.01$) or triple asterisks ($P < 0.001$, Student's *t* test). C, Venn diagrams of hypo-CG, -CHG, and -CHH DMRs and DMGs in *osddm1a/1b* and *osdrum2*. D, Box plots of CHH methylation levels of overlapped and nonoverlapped hypo-CHH DMRs in wild-type (WT) plants (left) and CHH methylation losses of overlapped hypo-CHH DMRs and nonoverlapped DMRs in *osdrum2* and *osddm1a/1b* plants (right). Significant differences are indicated by triple asterisks ($P < 0.001$, Student's *t* test). E, CHH methylation level changes (*y* axis; in minus percentage) of each bin (1 kb) with differential 24- and 21-nucleotide siRNA levels (*x* axis; false discovery rate < 0.01 , Student's *t* test) in *osdrum2* compared with the wild type.



regions displayed more significant losses of CHH methylation in both *osdrum2* and *osddm1a/1b* compared with nonoverlapped regions (Fig. 5D). We noted that the decreases of CHH methylation were more important in *osdrum2* than in *osddm1a/1b* (Fig. 5D). Slight decreases of CHH methylation of nonoverlapped regions also could be detected in *osddm1a/1b* plants (Fig. 5D). These data suggest that *OsDDM1* and *OsDRM2* may cooperate for high levels of CHH methylation in the rice genome.

Given the intrinsic relationship between DRM2-mediated DNA methylation and small RNAs, we conducted small RNA sequencing (RNA-seq) of *osdrum2* plants using the same tissues as for the BS-seq. About 30 million reads for the wild type and 44 million reads for *osdrum2* were obtained. In total, 17,932 (15,189 down-regulated and 2,743 up-regulated) differential 24-nucleotide siRNA regions were identified between

the wild type and *osdrum2*, indicating that *OsDRM2* was required for the production of a large number of siRNAs. To explore a possible relationship between the regional abundance of siRNAs and hypo-CHH DMRs found in *osdrum2*, we binned the abundance of 24- and 21-nucleotide siRNAs into 1-kb windows in the genome (as for DMRs) and searched for differences between the wild type and *osdrum2*. We plotted the differential 24- and 21-nucleotide siRNA regions (false discovery rate < 0.01) that were at the same time *osdrum2* hypo-CHH DMRs ($P \leq 0.01$) in terms of relative siRNA abundance (*x* axis) and DNA methylation levels in *osdrum2* versus the wild type (*y* axis; Fig. 5E). We found that a majority of hypo-CHH DMRs showed reduced 24-nucleotide siRNA levels in *osdrum2*, indicating a positive correlation between the 24-nucleotide siRNA abundance and *OsDRM2*-mediated CHH methylation.

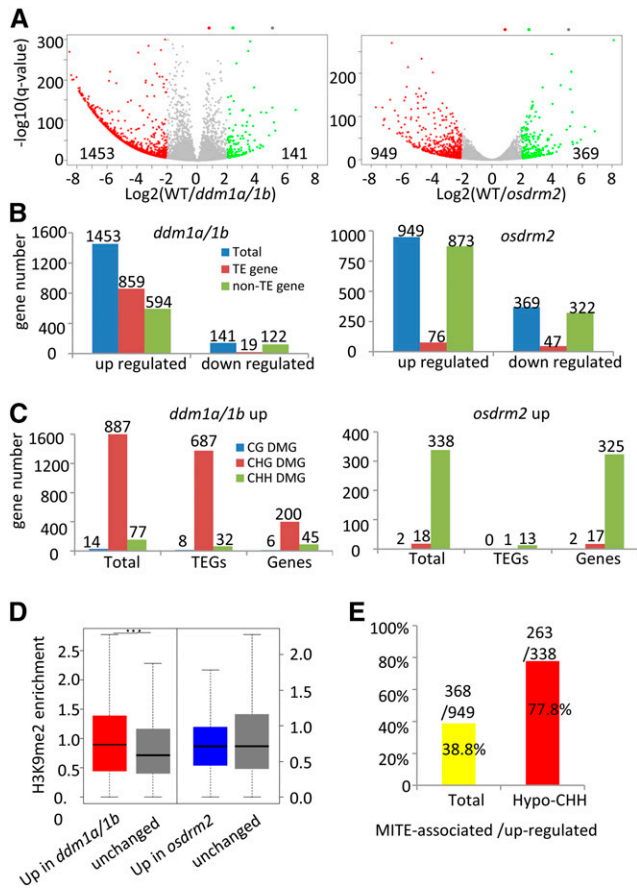


Figure 6. Differentially expressed protein-coding genes and TEGs in *osddm1a/1b* and *osdrm2* mutants. A, Total numbers of differentially expressed genes (greater than 4-fold; $P < 0.01$) in *osddm1a/1b* and *osdrm2* compared with the wild type (WT). B, Numbers of up- and down-regulated protein-coding genes and TEGs in the mutants. C, Numbers of up-regulated protein-coding genes and TEGs that are at the same time hypo-CG, -CHG, and -CHH DMGs in *osddm1a/1b* and *osdrm2*. D, Relative enrichment of H3K9me2 of up-regulated genes compared with unaffected genes in *osddm1a/1b* and *osdrm2*. Significant enrichments are indicated by triple asterisks ($P < 0.001$, Student's *t* test). E, Most of the up-regulated and hypo-CHH DMGs are associated with MITEs.

Effects of the *osddm1a/1b* and *osdrm2* Mutations on Gene Expression

To study the mutation effects of *osddm1a/1b* and *osdrm2* on gene expression, we analyzed the transcriptomes of the same tissues by RNA-seq (Supplemental Table S4). Two biological repeats were analyzed for both the wild type and the mutants. The sequence data displayed a high reproducibility ($r^2 > 0.99$; Supplemental Fig. S6A). Analysis of the data revealed 1,453 up-regulated and 141 down-regulated genes in *osddm1a/1b* and 949 up-regulated and 369 down-regulated genes in *osdrm2* compared with the wild type (greater than 4-fold; $P < 0.001$; Fig. 6, A and B). The many more up-regulated than down-regulated genes found in the mutants highlighted the repressive

function of OsDDM1 and OsDRM2 in gene repression. In *osddm1a/1b*, about 60% (859 of 1,453) of the up-regulated genes were TEGs (Fig. 6C), among which 80.3% (687 of 859) were hypo-CHG DMGs, compared with about 1% (eight of 859) and 3.7% (32 of 859) of the up-regulated hypo-CG or hypo-CHH methylated TEGs, respectively (Fig. 6C). Quantitative reverse transcription (qRT)-PCR analysis of five TEGs that lost methylation confirmed the data (Supplemental Figs. S3 and S7A). These data suggested that OsDDM1-mediated methylation was required for the repression of TEGs. Moreover, the up-regulated protein-coding genes were more enriched for H3K9me2 than unaffected genes (Fig. 6D). About 34% (200 of 594) of the up-regulated protein-coding genes were hypo-CHG DMGs, compared with only 1% (six of 594) hypo-CG and 8% (45 of 594) hypo-CHH DMGs (Fig. 6C; Supplemental Data Set S1). qRT-PCR analysis of the five **protein-coding** genes that lost methylation confirmed the data (Supplemental Figs. S3 and S7B). These results indicated that OsDDM1-mediated CHG methylation was required for the repression of TEGs as well as a subset of protein-coding genes that display heterochromatic features.

By contrast, in *osdrm2* plants, most (873 of 949) up-regulated genes were protein-coding genes (Fig. 6B). About 36% (338 of 949) of up-regulated genes were hypo-CHH DMGs (Fig. 6C; Supplemental Data Set S1). There were very few or no up-regulated hypo-CHG or hypo-CG DMGs. qRT-PCR analysis of the four genes that lost CHH methylation in the mutant confirmed the data (Supplemental Figs. S3 and S7C). Most (263 of 338) of the hypo-CHH methylated and up-regulated genes were associated with MITEs (Fig. 6E), supporting the assumption that OsDRM2 targeted MITEs for genic CHH methylation and gene repression.

DISCUSSION

Our data indicate that the two *OsDDM1* genes have redundant functions in rice genome-wide DNA methylation, which differs in several respects from that of Arabidopsis *DDM1*. First, our results show that OsDDM1 plays an essential role in gene regulation and plant growth, as the loss of OsDDM1 function produced very severe growth defects in the first generation, while Arabidopsis *ddm1* mutants grew relatively normally in the initial generations and produced developmental abnormalities only after multiple rounds of self-pollination (Kakutani et al., 1996). These gradually developed abnormalities are mainly due to the insertion of derepressed TEs or the rearrangement of repeats during generational propagation (Miura et al., 2001; Singer et al., 2001; Tsukahara et al., 2009; Yi and Richards, 2009), although others are due to DNA methylation changes that affect gene expression (Soppe et al., 2000; Saze and Kakutani, 2007). Maize also has two DDM1 orthologs, *Chr101* and *Chr106*. While single gene loss-of-function alleles are viable, double mutation

is likely lethal, as no double mutant could be obtained (Li et al., 2014). Those results together with our data suggest that the loss of DDM1 genes in grasses may have stronger deleterious phenotypic effects than in Arabidopsis.

The developmental defects of *osddm1a/1b* plants are likely due to the alteration of epigenetic changes of many protein-coding genes. OsDDM1-dependent DNA methylation is likely to be involved directly in the epigenetic repression of functional genes in rice, as many derepressed genes in *osddm1a/1b* have been shown to be involved in rice development and growth (Supplemental Data Set S1). Among these genes, we checked DNA methylation and transcript levels of *OsFIE1*, *OsMPS*, *Kala4*, and several others (Supplemental Figs. S3 and S7B). *OsFIE1* encodes a key component of POLYCOMB REPRESSIVE COMPLEX2 and is repressed in rice vegetative tissues. Loss of DNA methylation from *OsFIE1* during tissue culture leads to stable derepression of the gene, which severely affects rice plant growth, leading to a dwarf phenotype (Zhang et al., 2012). Overexpression of *OsMPS* also resulted in decreased plant stature (Schmidt et al., 2013). *Kala4* encodes a basic helix-loop-helix protein whose ectopic expression produces black grains (Oikawa et al., 2015), which also were observed in *osddm1a/1b* (Supplemental Fig. S1E). The function of OsDDM1 in maintaining the proper expression pattern of a large number of genes may be related at least partly to DNA methylation in genic regions. However, it is not ruled out that some of the phenotypes also may be caused by the derepression of TEs during the production of the double mutants. A relatively high cooccurrence between hypo-CHG DMG and up-regulated genes suggested that OsDDM1-mediated CHG methylation played an important role in developmental gene repression (Fig. 6C). However, only 8% of the up-regulated genes were hypo-CHH DMGs in *osddm1a/1b*, and only about 20% of the up-regulated genes (greater than 2-fold; $P < 0.01$) in *osddm1a/1b* overlapped with those in *osdrm2* (Supplemental Fig. S6B). This could be explained by relatively low levels of decreases of CHH methylation in *osddm1a/1b* (Figs. 1, B and D, and 2).

The Arabidopsis *ddm1* mutation mostly reduces methylation in all sequence contexts of heterochromatic repeats, TEs, and TEGs, but it produces ectopic CHG methylation in gene bodies (Lippman et al., 2004; Zemach et al., 2013). However, our data indicate that, among the three sequence contexts, CHG methylation was affected mostly by the *osddm1a/1b* mutation. Similarly, loss-of-function alleles of one maize DDM1 gene, *Chr106*, also results in more reduction of non-CG than CG methylation (Li et al., 2014). It is established that CHG methylation and H3K9me2 form a positive feedback loop in Arabidopsis: CHG methylation by CMT3 requires H3K9me2, to which CMT3 binds via its chromo- and bromo-adjacent homology domains (Law and Jacobsen, 2010; Du et al., 2012). H3K9 dimethylation by SUVH proteins requires CHG methylation, to which SUVH proteins bind via the SRA domain

(Johnson et al., 2007; Rajakumara et al., 2011). CHG methylation is kept out of genes by a histone demethylase, IBM1, which removes H3K9me2 from gene bodies (Saze and Kakutani, 2011). It seemed that CHG methylation loss in *osddm1a/1b* plants was not due to up-regulation of the rice homolog of IBM1 (*JMJ719*) or repression of *OsCMT3* or *OsCMT2*, as their transcript levels were not clearly altered in the mutant (Supplemental Fig. S6D). The more important role of OsDDM1 in heterochromatic CHG methylation suggests that OsDDM1-mediated chromatin remodeling is essential to facilitate the *OsCMT3*-mediated CHG methylation of heterochromatic regions of the rice genome (Cheng et al., 2015).

In Arabidopsis, RdDM operates primarily through DRM2 and is responsible for a relatively minor fraction of genomic CHH methylation (Wierzbicki et al., 2012; Zemach et al., 2013), and CMT2 mediates most CHH methylation, separately from the RdDM pathway (Zemach et al., 2013). It has been shown that Arabidopsis DDM1 facilitates CMT2-mediated CHH methylation in body regions of long (or heterochromatic) TEs, while RdDM-dependent CHH methylation mostly targets short TEs and TE edges (Zemach et al., 2013). Our data here suggest that OsDDM1 may be involved in OsDRM2-mediated CHH methylation at genic regions (Fig. 5C). OsDDM1 may facilitate OsDRM2 or RdDM-mediated CHH methylation in the rice genome by the remodeling of dispersed small heterochromatin in genic regions by displacing histone H1 (Zemach et al., 2013). However, it is possible that the loss of CHH methylation is coordinated with that of CHG in *osddm1a/1b*, as observed in Arabidopsis and maize (Li et al., 2014; Stroud et al., 2014).

Our data indicate that, in rice, CHH methylation was located essentially in the euchromatic regions of the genome (Fig. 1B), in agreement with the previous observations that CHH peaks are absent in the rice pericentromeric regions, in contrast to the more localized pattern of repeats close to centromeres in Arabidopsis (Feng et al., 2010). It is believed that this might reflect the fact that repeats are widely spread across the rice genome (Feng et al., 2010). The massive loss of CHH methylation (about 85%; Table I) in *osdrm2* plants suggests that the OsDRM2-mediated RdDM pathway in rice may play a major role for CHH methylation. Our results indicate that, in fact, rice CHH methylation essentially targets small TEs such as MITEs that are largely scattered in euchromatic regions, most at the 5' and 3' ends of genes. MITE-associated genes that have significantly lower level expression than genes away from MITEs (Lu et al., 2012) are likely to be repressed by OsDRM2-mediated CHH methylation, as a large portion of up-regulated genes were MITE-associated hypo-CHH DMGs in *osdrm2* (Fig. 6). This suggests an important role of *OsDRM2* and RdDM in gene regulation in rice. Many up-regulated DMGs were important rice developmental genes, such as *OsGA2ox5* and *Os08g19420* (Supplemental Data Set S1). The overexpression of *OsGA2ox5* produces a severe dwarf

phenotype (Shan et al., 2014), and plants with increased expression of Os08g19420 showed exaggerated flag leaf angle at the heading stage (Wei et al., 2014). These phenotypes were observed in *osdrm2* (Fig. 1A; Supplemental Fig. S1F). Interestingly, *OsMPS*, hypo-CHH methylated and up-regulated in *osddm1a/1b*, also was hypo-CHH methylated and up-regulated in *osdrm2* (Supplemental Figs. S3 and S6, B and C). RdDM is a DNA methylation process triggered by double-stranded RNA from which siRNAs are generated and used by the RNA interference machinery to guide DRM2-mediated DNA methylation. Conversely, the production of siRNA also depends on DRM2 (Zilberman et al., 2004; Henderson et al., 2010). The correlation between the decrease of 24-nucleotide siRNA abundance and the loss of CHH methylation in *osdrm2* suggests that OsDRM2 is required for siRNA production in the RdDM pathway that regulates many protein-coding genes in rice. This hypothesis is supported by hundreds of up-regulated genes and the severe phenotypes of *osdrm2* mutants and those of other rice RdDM genes, such as *OsDCL3a*, *OsDCL4*, and *OsRDR6* (Wu et al., 2010; Song et al., 2012a, 2012b; Arikrit et al., 2013). By comparison, mutants of the Arabidopsis homologous genes display no or only subtle phenotypes (Cao and Jacobsen, 2002), whereas no double mutants of the maize DRM2 orthologs *Zmet3* and *Zmet7* could be recovered (Li et al., 2014). Likely, DNA methylation mediated by DRM2-like proteins in grasses is crucial for normal plant growth and viability.

These specific features of OsDDM1 and OsDRM2 in DNA methylation and epigenetic regulation of gene expression, together with both the conserved and specific functions of OsMET1 in DNA methylation (Hu et al., 2014), indicate that the precise functions of DNA methylation regulators and the identities of rice pathways that mediate the bulk of methylation of the rice genome differ from those in Arabidopsis. The distinct feature of the rice DNA methylation pattern and the unique roles of OsDDM1 and OsDRM2 may be related to the differences in genome and chromatin organization of rice and Arabidopsis. The majority of CHH methylation locates in euchromatic regions in rice (Fig. 1B), whereas most CHH methylation is in the pericentromeric heterochromatin in Arabidopsis (Lister et al., 2008; Stroud et al., 2014). This is likely due to the fact that heterochromatic regions are relatively dispersed across chromosomes in rice but are much more focused in pericentromeric regions in Arabidopsis.

MATERIALS AND METHODS

Plant Materials

Rice (*Oryza sativa* L. ssp. *japonica* 'DongJin') plants were used in this study. T-DNA insertion lines of *osddm1a* (PFG_3A-51065), *osddm1b* (PFG_2B-60109), and *osdrm2* (PFG_3A-04110) were obtained from the Postech rice mutant database (<http://www.postech.ac.kr/life/pfg/risd/>). The homozygous mutants of *osddm1a*, *osddm1b*, *osdrm2*, *osddm1a/1b* double mutant, *osddm1a/1b/osdrm2* triple mutant, and callus culture-regenerated wild type were germinated and

grown on hormone-free, one-half-strength Murashige and Skoog medium under 16/8 h of light/dark at 30°C/25°C or in the field. Twelve-day-old seedling leaves from each genotype were harvested for chromatin, genomic DNA, or total RNA extraction.

Genotyping of *osddm1a*, *osddm1b*, and *osdrm2* Plants

The insertion of *osddm1a* was confirmed by PCR using the primers 3A-51065-P1 and 3A-51065-P2 and the T-DNA-specific primer P3, the *osddm1b* mutant by the primers 2B-60109-P1 and 2B-60109-P2 and the T-DNA-specific primer P3, and the *osdrm2* mutant by the primers 3A-04110-P1 and 3A-04110-P2 and the T-DNA-specific primer P4. The primers used for genotyping and reverse transcription-PCR analysis are listed in Supplemental Data Set S2.

Semiquantitative Reverse Transcription-PCR and qRT-PCR Analysis

Total RNA was isolated from 12-d-old seedling leaves using TRIzol reagent (Invitrogen/Life Technologies). Four micrograms of treated total RNA was used to synthesize first-strand complementary DNA with a reverse transcription kit (Promega). The rice *Actin* gene was used as an internal control.

Methylation-Sensitive Endonuclease Digestion

Genomic DNA (1 μ g) isolated from 12-d-old seedlings was digested with 40 units of the methylation-sensitive restriction enzyme *McrBC* (New England Biolabs; M0272L) for 6 h, which cuts methylated DNA, followed by PCR with specific primer pairs (Supplemental Data Set S2).

Enzymatic Hydrolysis of DNA and Liquid Chromatography-Mass Spectrometry Analysis

Enzymatic hydrolysis of DNA and liquid chromatography-mass spectrometry analysis were conducted according to protocols described previously, with slight modifications (Friso et al., 2002). DNA was extracted from mature leaves using the DNeasy plant mini kit (Qiagen). About 0.5 μ g of DNA was denatured by heating at 100°C for 3 min and subsequently chilled in ice slush. One-tenth volume of 0.1 M ammonium acetate (pH 5.3) and 2 units of benzonase P1 (Sigma) were added and incubated at 37°C for 2 h. To the solution were subsequently added one-tenth volume of 1 M ammonium bicarbonate (Sigma) and 0.002 units of venom phosphodiesterase I (Sigma). The incubation was continued for an additional 2 h at 37°C. Thereafter, the mixture was incubated for 1 h at 37°C with 0.5 units of alkaline phosphatase (New England Biolabs). After digestion, 0.4 mL of ultrapure water filtered through a 0.22- μ m filter for liquid chromatography-mass spectrometry analysis was added. Nucleoside standards including deoxycytidine and 5-methyldeoxycytidine were used to determine the peak position of each nucleoside.

Chromatin Immunoprecipitation

Chromatin was isolated from 2 g of rice seedling leaves. After sonication, chromatin fragments were incubated with antibody (anti-H3K9me2 or anti-H3K27me3)-coated beads (Invitrogen/Life Technologies; 10001D) overnight. After wash and elution, products were reverse cross-linked. Then, the products were treated with protease K (Takara; 9034). Anti-H3K9me2 (ab1220; Abcam) and anti-H3K27me3 (A2363; Abclonal) antibodies were used.

Whole-Genome BS-Seq Library Construction and Sequencing

For genomic BS-seq, the total genomic DNA of callus culture-regenerated wild-type and mutant plants was extracted from 12-d-old seedling leaves using the DNeasy plant mini kit (Qiagen). The library was prepared and sequenced at the Novogene Bioinformatics Institute on an Illumina HiSeq 2500 platform.

BS-Seq Data Processing

Quality control, mapping, and processing of BS-seq reads were performed as follows. Briefly, low-quality reads were removed from raw data by

Trimmomatic (<http://www.usadellab.org/cms/uploads/supplementary/Trimmomatic/Trimmomatic-Src-0.35.zip>), and then the clean data were mapped to the MSU7.0 rice reference genome (ftp://ftp.plantbiology.msu.edu/pub/data/Eukaryotic_Projects/o_sativa/annotation_dbs/pseudomolecules/version_7.0/all.dir/) by BatMeth (Lim et al., 2012). Only uniquely mapped reads were retained for further analysis. To calculate the methylation density, we first counted the total number of nucleotides C and T that overlap with each genomic cytosine site across the whole genome. The methylation level for each cytosine site was calculated by the sequencing depth of this site divided by the number of unconverted cytosines.

Identification of DMCs, DMRs, and DMGs

The DMCs between any two genotypes were defined by a binomial test (methylSig; Park et al., 2014). Only cytosine sites whose adjusted q values were 0.01 or less and had DNA methylation differences of 0.7, 0.5, or 0.1 between any two genotypes were designated as DMCs (Stroud et al., 2013). The DMRs were discriminated by comparison of the methylation levels of 1-kb windows/regions throughout the genome between any two genotypes. For the identification of DMGs, either the methylation level of the gene body or 2-kb upstream flanks (promoter) of the gene has a difference (calculated the same as DMCs).

mRNA Sequencing and Small RNA-Seq and Analysis

Total RNA was extracted from 12-d-old seedlings using TRIzol reagent (Invitrogen). RNA-seq libraries were constructed from total RNA isolated using TRIzol reagent (Invitrogen/Life Technologies) from leaf tissues. Total RNA (10 μ g) for each sample was used to purify poly(A) mRNA; this mRNA was used for the synthesis and amplification of complementary DNA. The RNA-seq libraries were prepared using the TruSeq RNA Sample Preparation Kit from Illumina. Libraries were sequenced on an Illumina HiSeq 2000.

Small RNA-seq libraries were constructed from total RNAs isolated from the same tissues as for the mRNA libraries, using the TruSeq Small RNA Sample Preparation Kit from Illumina. The libraries were sequenced on the same Illumina HiSeq 2000 as the mRNA sequencing libraries.

RNA-seq data were first cleaned by removing contaminations and low-quality reads by Trimmomatic (<http://www.usadellab.org/cms/uploads/supplementary/Trimmomatic/Trimmomatic-Src-0.35.zip>). The clean data were mapped against the MSU7.0 rice genome with corresponding annotation by Tophat2.0 (Kim et al., 2013; <http://tophat.cbcb.umd.edu/>) using default parameters. Then, the gene counts were calculated with htseq-count, and the differentially expressed genes (\log [fold change] ≥ 2 , $q < 0.05$) were calculated by DESeq2.

Small RNA sequence raw data were cleaned by removing adaptor contamination and low-quality reads by Cutadapt (Martin, 2011). MicroRNA (<http://www.mirbase.org/ftp.shtml>), transfer RNA (http://rice.plantbiology.msu.edu/analyses_search_tRNA.shtml), ribosomal RNA (Rice Genome Annotation MSU7.0), small nucleolar RNA, and small nuclear RNA (http://www.arb-silva.de/no_cache/download/archive/release_111/Exports/) also were removed. Clean reads were aligned to the rice MSU7.0 reference genome by Bowtie (Langmead et al., 2009), allowing zero mismatches and unique mapping. Two types of small RNA abundance were calculated by 21- or 24-nucleotide read numbers falling into 1-kb windows/regions throughout the whole genomes, and windows containing more than three reads were tested by edgeR (Robinson et al., 2010) between samples. Windows with corrected $P \leq 0.01$ were defined as differential small RNA regions.

Chromatin Immunoprecipitation Sequencing and Analysis

DNA from chromatin immunoprecipitation was used to construct sequencing libraries following the protocol provided by the Illumina TruSeq ChIP Sample Prep Set A and sequenced by HiSeq 2000.

Trimmomatic (version 0.32) was used to filter out low-quality reads and crop all reads to a uniform length (45bp). Clean reads were mapped to the rice genome (Rice Genome Annotation Project version 7) by default, allowing up to two mismatches using Bowtie2 (version 2.1.0).

The sequence data and analyses generated in this work have been submitted to the National Center for Biotechnology Information databases under the accession number GSE81436.

Supplemental Data

The following supplemental materials are available.

Supplemental Figure S1. Characterization of expression and T-DNA insertion mutants of *OsDDM1a*, *OsDDM1b*, and *OsDRM2*.

Supplemental Figure S2. Cytosine methylation average levels in all sequence contexts in TEGs.

Supplemental Figure S3. Genome browser and validation of DNA methylation loss in the mutants.

Supplemental Figure S4. Patterns of cytosine methylation (CG, CHG, and CHH) of additional TEs and repeats in the wild type and *osddm1a*, *osddm1b*, *osddm1a/1b*, and *osdrm2* mutants.

Supplemental Figure S5. Heterochromatin localization of hyper-CHH methylated TEs in *osddm1a/1b* plants.

Supplemental Figure S6. Transcriptomic analysis.

Supplemental Figure S7. Transcript levels (relative to *Actin1*) tested by qRT-PCR.

Supplemental Table S1. Cytosine methylation levels in wild-type and mutant rice leaves measured by mass spectrometry.

Supplemental Table S2. BS-seq data of the wild type and mutants (two repeats per sample).

Supplemental Table S3. H3K27me3 and H3K9me2 chromatin immunoprecipitation sequencing data.

Supplemental Table S4. RNA-seq data.

Supplemental Table S5. Numbers of hypo- or hyper-DMCs, DMRs, and DMGs in CG, CHG, and CHH contexts in the mutants.

Supplemental Data Set S1. Differentially methylated and differentially expressed genes in *osddm1* and *osdrm2* mutants.

Supplemental Data Set S2. Sequences of primers used in this study.

ACKNOWLEDGMENTS

We thank Dengnian Liu for the initial work in *OsDDM1* and Dr. Qinghua Zhang for sequencing using Illumina HiSeq 2000.

Received March 8, 2016; accepted May 11, 2016; published May 12, 2016.

LITERATURE CITED

- Arikit S, Zhai J, Meyers BC (2013) Biogenesis and function of rice small RNAs from non-coding RNA precursors. *Curr Opin Plant Biol* **16**: 170–179
- Brzeski J, Jerzmanowski A (2003) Deficient in DNA methylation 1 (DDM1) defines a novel family of chromatin-remodeling factors. *J Biol Chem* **278**: 823–828
- Bureau TE, Wessler SR (1994) Mobile inverted-repeat elements of the Tourist family are associated with the genes of many cereal grasses. *Proc Natl Acad Sci USA* **91**: 1411–1415
- Cao X, Jacobsen SE (2002) Role of the Arabidopsis DRM methyltransferases in de novo DNA methylation and gene silencing. *Curr Biol* **12**: 1138–1144
- Chen X, Zhou DX (2013) Rice epigenomics and epigenetics: challenges and opportunities. *Curr Opin Plant Biol* **16**: 164–169
- Cheng C, Tarutani Y, Miyao A, Ito T, Yamazaki M, Sakai H, Fukai E, Hirochika H (2015) Loss of function mutations in the rice chromomethylase *OscMT3a* cause a burst of transposition. *Plant J* **83**: 1069–1081
- Cheng Z, Buell CR, Wing RA, Gu M, Jiang J (2001) Toward a cytological characterization of the rice genome. *Genome Res* **11**: 2133–2141
- Du J, Zhong X, Bernatavichute YV, Stroud H, Feng S, Caro E, Vashisht AA, Terragni J, Chin HG, Tu A, et al (2012) Dual binding of chromomethylase domains to H3K9me2-containing nucleosomes directs DNA methylation in plants. *Cell* **151**: 167–180

- Feng S, Cokus SJ, Zhang X, Chen PY, Bostick M, Goll MG, Hetzel J, Jain J, Strauss SH, Halpern ME, et al (2010) Conservation and divergence of methylation patterning in plants and animals. *Proc Natl Acad Sci USA* **107**: 8689–8694
- Feschotte C, Wessler SR (2002) Mariner-like transposases are widespread and diverse in flowering plants. *Proc Natl Acad Sci USA* **99**: 280–285
- Friso S, Choi SW, Dolnikowski GG, Selhub J (2002) A method to assess genomic DNA methylation using high-performance liquid chromatography/electrospray ionization mass spectrometry. *Anal Chem* **74**: 4526–4531
- Gent JL, Madzima TF, Bader R, Kent MR, Zhang X, Stam M, McGinnis KM, Dawe RK (2014) Accessible DNA and relative depletion of H3K9me2 at maize loci undergoing RNA-directed DNA methylation. *Plant Cell* **26**: 4903–4917
- He G, Zhu X, Elling AA, Chen L, Wang X, Guo L, Liang M, He H, Zhang H, Chen F, et al (2010) Global epigenetic and transcriptional trends among two rice subspecies and their reciprocal hybrids. *Plant Cell* **22**: 17–33
- Henderson IR, Deleris A, Wong W, Zhong X, Chin HG, Horwitz GA, Kelly KA, Pradhan S, Jacobsen SE (2010) The de novo cytosine methyltransferase DRM2 requires intact UBA domains and a catalytically mutated paralogue DRM3 during RNA-directed DNA methylation in *Arabidopsis thaliana*. *PLoS Genet* **6**: e1001182
- Higo H, Tahir M, Takashima K, Miura A, Watanabe K, Tagiri A, Ugaki M, Ishikawa R, Eiguchi M, Kurata N, et al (2012) DDM1 (decrease in DNA methylation) genes in rice (*Oryza sativa*). *Mol Genet Genomics* **287**: 785–792
- Hu L, Li N, Xu C, Zhong S, Lin X, Yang J, Zhou T, Yuliang A, Wu Y, Chen YR, et al (2014) Mutation of a major CG methylase in rice causes genome-wide hypomethylation, dysregulated genome expression, and seedling lethality. *Proc Natl Acad Sci USA* **111**: 10642–10647
- Jeddeloh JA, Stokes TL, Richards EJ (1999) Maintenance of genomic methylation requires a SWI2/SNF2-like protein. *Nat Genet* **22**: 94–97
- Johnson LM, Bostick M, Zhang X, Kraft E, Henderson I, Callis J, Jacobsen SE (2007) The SRA methyl-cytosine-binding domain links DNA and histone methylation. *Curr Biol* **17**: 379–384
- Kakutani T, Jeddeloh JA, Flowers SK, Munakata K, Richards EJ (1996) Developmental abnormalities and epimutations associated with DNA hypomethylation mutations. *Proc Natl Acad Sci USA* **93**: 12406–12411
- Kim D, Pertea G, Trapnell C, Pimentel H, Kelley R, Salzberg SL (2013) TopHat2: accurate alignment of transcriptomes in the presence of insertions, deletions and gene fusions. *Genome Biol* **14**: R36
- Langmead B, Trapnell C, Pop M, Salzberg SL (2009) Ultrafast and memory-efficient alignment of short DNA sequences to the human genome. *Genome Biol* **10**: R25
- Law JA, Jacobsen SE (2010) Establishing, maintaining and modifying DNA methylation patterns in plants and animals. *Nat Rev Genet* **11**: 204–220
- Li Q, Eichten SR, Hermanson PJ, Zaunbrecher VM, Song J, Wendt J, Rosenbaum H, Madzima TF, Sloan AE, Huang J, et al (2014) Genetic perturbation of the maize methylome. *Plant Cell* **26**: 4602–4616
- Li X, Zhu J, Hu F, Ge S, Ye M, Xiang H, Zhang G, Zheng X, Zhang H, Zhang S, et al (2012) Single-base resolution maps of cultivated and wild rice methylomes and regulatory roles of DNA methylation in plant gene expression. *BMC Genomics* **13**: 300
- Lim JQ, Tennakoon C, Li G, Wong E, Ruan Y, Wei CL, Sung WK (2012) BatMeth: improved mapper for bisulfite sequencing reads on DNA methylation. *Genome Biol* **13**: R82
- Lippman Z, Gendrel AV, Black M, Vaughn MW, Dedhia N, McCombie WR, Lavine K, Mittal V, May B, Kasschau KD, et al (2004) Role of transposable elements in heterochromatin and epigenetic control. *Nature* **430**: 471–476
- Lister R, O'Malley RC, Tonti-Filippini J, Gregory BD, Berry CC, Millar AH, Ecker JR (2008) Highly integrated single-base resolution maps of the epigenome in *Arabidopsis*. *Cell* **133**: 523–536
- Liu X, Zhou S, Wang W, Ye Y, Zhao Y, Xu Q, Zhou C, Tan F, Cheng S, Zhou DX (2015) Regulation of histone methylation and reprogramming of gene expression in the rice inflorescence meristem. *Plant Cell* **27**: 1428–1444
- Lu C, Chen J, Zhang Y, Hu Q, Su W, Kuang H (2012) Miniature inverted-repeat transposable elements (MITEs) have been accumulated through amplification bursts and play important roles in gene expression and species diversity in *Oryza sativa*. *Mol Biol Evol* **29**: 1005–1017
- Martin M (2011) Cutadapt removes adapter sequences from high-throughput sequencing reads. *EMBnet journal* **17**: 10–12
- Miura A, Yonebayashi S, Watanabe K, Toyama T, Shimada H, Kakutani T (2001) Mobilization of transposons by a mutation abolishing full DNA methylation in *Arabidopsis*. *Nature* **411**: 212–214
- Moritoh S, Eun CH, Ono A, Asao H, Okano Y, Yamaguchi K, Shimatani Z, Koizumi A, Terada R (2012) Targeted disruption of an orthologue of DOMAINS REARRANGED METHYLASE 2, OsDRM2, impairs the growth of rice plants by abnormal DNA methylation. *Plant J* **71**: 85–98
- Oikawa T, Maeda H, Oguchi T, Yamaguchi T, Tanabe N, Ebana K, Yano M, Ebitani T, Izawa T (2015) The birth of a black rice gene and its local spread by introgression. *Plant Cell* **27**: 2401–2414
- Park Y, Figueroa ME, Rozek LS, Sartor MA (2014) MethylSig: a whole genome DNA methylation analysis pipeline. *Bioinformatics* **30**: 2414–2422
- Paterson AH, Bowers JE, Bruggmann R, Dubchak I, Grimwood J, Gundlach H, Haberler G, Hellsten U, Mitros T, Poliakov A, et al (2009) The Sorghum bicolor genome and the diversification of grasses. *Nature* **457**: 551–556
- Rajakumara E, Law JA, Simanshu DK, Voigt P, Johnson LM, Reinberg D, Patel DJ, Jacobsen SE (2011) A dual flip-out mechanism for 5mC recognition by the *Arabidopsis* SUVH5 SRA domain and its impact on DNA methylation and H3K9 dimethylation in vivo. *Genes Dev* **25**: 137–152
- Robinson MD, McCarthy DJ, Smyth GK (2010) edgeR: a Bioconductor package for differential expression analysis of digital gene expression data. *Bioinformatics* **26**: 139–140
- Saze H, Kakutani T (2007) Heritable epigenetic mutation of a transposon-flanked *Arabidopsis* gene due to lack of the chromatin-remodeling factor DDM1. *EMBO J* **26**: 3641–3652
- Saze H, Kakutani T (2011) Differentiation of epigenetic modifications between transposons and genes. *Curr Opin Plant Biol* **14**: 81–87
- Schmidt R, Schippers JH, Mieulet D, Obata T, Fernie AR, Guiderdoni E, Mueller-Roeber B (2013) MULTIPASS, a rice R2R3-type MYB transcription factor, regulates adaptive growth by integrating multiple hormonal pathways. *Plant J* **76**: 258–273
- Shan C, Mei Z, Duan J, Chen H, Feng H, Cai W (2014) OsGA2ox5, a gibberellin metabolism enzyme, is involved in plant growth, the root gravity response and salt stress. *PLoS ONE* **9**: e87110
- Singer T, Yordan C, Martienssen RA (2001) Robertson's Mutator transposons in *A. thaliana* are regulated by the chromatin-remodeling gene *Decrease in DNA Methylation (DDM1)*. *Genes Dev* **15**: 591–602
- Song X, Li P, Zhai J, Zhou M, Ma L, Liu B, Jeong DH, Nakano M, Cao S, Liu C, et al (2012a) Roles of DCL4 and DCL3b in rice phased small RNA biogenesis. *Plant J* **69**: 462–474
- Song X, Wang D, Ma L, Chen Z, Li P, Cui X, Liu C, Cao S, Chu C, Tao Y, et al (2012b) Rice RNA-dependent RNA polymerase 6 acts in small RNA biogenesis and spikelet development. *Plant J* **71**: 378–389
- Soppe WJ, Jacobsen SE, Alonso-Blanco C, Jackson JP, Kakutani T, Koornneef M, Peeters AJ (2000) The late flowering phenotype of *fwa* mutants is caused by gain-of-function epigenetic alleles of a homeodomain gene. *Mol Cell* **6**: 791–802
- Stroud H, Ding B, Simon SA, Feng S, Bellizzi M, Pellegrini M, Wang GL, Meyers BC, Jacobsen SE (2013) Plants regenerated from tissue culture contain stable epigenome changes in rice. *eLife* **2**: e00354
- Stroud H, Do T, Du J, Zhong X, Feng S, Johnson L, Patel DJ, Jacobsen SE (2014) Non-CG methylation patterns shape the epigenetic landscape in *Arabidopsis*. *Nat Struct Mol Biol* **21**: 64–72
- Tao Y, Xi S, Briones V, Muegge K (2010) Lsh mediated RNA polymerase II stalling at HoxC6 and HoxC8 involves DNA methylation. *PLoS ONE* **5**: e9163
- Tran RK, Zilberman D, de Bustos C, Ditt RF, Henikoff JG, Lindroth AM, Delrow J, Boyle T, Kwong S, Bryson TD, et al (2005) Chromatin and siRNA pathways cooperate to maintain DNA methylation of small transposable elements in *Arabidopsis*. *Genome Biol* **6**: R90
- Tsukahara S, Kobayashi A, Kawabe A, Mathieu O, Miura A, Kakutani T (2009) Bursts of retrotransposition reproduced in *Arabidopsis*. *Nature* **461**: 423–426
- Wei L, Gu L, Song X, Cui X, Lu Z, Zhou M, Wang L, Hu F, Zhai J, Meyers BC, et al (2014) Dicer-like 3 produces transposable element-associated 24-nt siRNAs that control agricultural traits in rice. *Proc Natl Acad Sci USA* **111**: 3877–3882

- Wierzbicki AT, Cocklin R, Mayampurath A, Lister R, Rowley MJ, Gregory BD, Ecker JR, Tang H, Pikaard CS (2012) Spatial and functional relationships among Pol V-associated loci, Pol IV-dependent siRNAs, and cytosine methylation in the Arabidopsis epigenome. *Genes Dev* **26**: 1825–1836
- Wu L, Zhou H, Zhang Q, Zhang J, Ni F, Liu C, Qi Y (2010) DNA methylation mediated by a microRNA pathway. *Mol Cell* **38**: 465–475
- Yi H, Richards EJ (2009) Gene duplication and hypermutation of the pathogen resistance gene SNC1 in the Arabidopsis bal variant. *Genetics* **183**: 1227–1234
- Zemach A, Kim MY, Hsieh PH, Coleman-Derr D, Eshed-Williams L, Thao K, Harmer SL, Zilberman D (2013) The Arabidopsis nucleosome remodeler DDM1 allows DNA methyltransferases to access H1-containing heterochromatin. *Cell* **153**: 193–205
- Zemach A, Kim MY, Silva P, Rodrigues JA, Dotson B, Brooks MD, Zilberman D (2010) Local DNA hypomethylation activates genes in rice endosperm. *Proc Natl Acad Sci USA* **107**: 18729–18734
- Zhang L, Cheng Z, Qin R, Qiu Y, Wang JL, Cui X, Gu L, Zhang X, Guo X, Wang D, et al (2012) Identification and characterization of an epi-allele of FIE1 reveals a regulatory linkage between two epigenetic marks in rice. *Plant Cell* **24**: 4407–4421
- Zilberman D, Cao X, Johansen LK, Xie Z, Carrington JC, Jacobsen SE (2004) Role of Arabidopsis ARGONAUTE4 in RNA-directed DNA methylation triggered by inverted repeats. *Curr Biol* **14**: 1214–1220